
The Channel Ratio Method of Scatter Correction for Radionuclide Image Quantitation

P. Hendrik Pretorius, Ado J. van Rensburg, Andries van Aswegen, Mattheus G. Lötter, Dawid E. Serfontein and Charles P. Herbst

Biophysics Department, University of the Orange Free State, Bloemfontein, South Africa

The accuracy of quantitation of radionuclide distributions in human tissue with the scintillation camera is decreased by attenuation and scatter of photons. If scatter correction is applied satisfactorily, narrow beam attenuation can be applied. In this article, a scatter correction technique, the channel ratio (CR) method, is introduced. The CR scatter correction method is proposed for quantitation of the radionuclide distribution in organs. The improvement in the geometrical resolution was measured and examples of clinical images are presented. In this method, the change in the ratio of counts from two symmetrical adjacent energy windows straddling the energy photopeak was used to eliminate the contribution of scattered photons during imaging with ^{99m}Tc . The theory and methods for the empirical affirmation are described. To apply the CR scatter correction method, two constants, the ratio of primary photons G and the ratio of scattered photons H in the same windows, were determined. Different sized sources in varying depths of water were imaged. When the source activities were quantified after scatter correction with the CR method, the measurements ranged from 96%–108% in comparison to the reference value in 100 mm water. The scatter fraction increased from 0.20 in 10 mm water to 1.44 in 200 mm water. The geometrical resolution expressed as full width at tenth maximum in 150 mm water improved by 30.4% and was restored to the value of the geometrical resolution in air. The CR scatter correction method is a simple method to correct for scatter in order to facilitate accurate quantitation of the radionuclide distribution during imaging with a scintillation camera.

J Nucl Med 1993; 34:330–335

The accuracy of absolute quantitation of radionuclide distributions in man with the scintillation camera is decreased by attenuation and scatter of photons (1). Many scattered photons travel in directions which allow them to pass through the collimator and be detected. Due to the 10%–15% full width at half maximum (FWHM) energy

resolution of the scintillation detector, only photons of ^{99m}Tc scattered through angles larger than 53° are eliminated when a 20% energy window is selected (2,3). The scattered photons not eliminated are included with the acquired data and degrade quantitative accuracy as well as the visual quality of the image. Different approaches were followed to reduce this effect. The value of the narrow beam attenuation coefficient was changed to that of broad beam geometry to compensate for the excess in scattered photons detected (1). A further significant improvement in quantitation of planar images was made with the introduction of the buildup factor approach (4–7). In this approach, the buildup factor was introduced to compensate for the scatter component of photons detected in an image. The buildup factor is a function of organ size and has to be determined to apply the technique.

The introduction of single-photon emission computed tomography (SPECT) enhanced the potential for quantitative data processing which required accurate scatter and attenuation correction. Several scatter correction methods were proposed which either measure (3,8–11), model (12, 13) or compute (2,14) the contribution of scatter. In all these methods, an improvement in the contrast and quantitative accuracy of images was reported (9–15). Some methods use an energy window for scattered photons and subtract a fraction of these counts from the photopeak counts (9–11,15). However, the published values of this fraction varies. The application of energy weighted acquisition (16–18) and Klein-Nishina energy corrections (19) were also proposed to reduce the effect of scattered photons. These methods are currently not available on all commercial cameras.

In this study, a scatter correction method, the channel ratio (CR) method, is introduced. In this method, the change in the ratio of counts obtained from two adjacent symmetrical windows straddling the photopeak is examined to determine and eliminate the contribution of scattered photons to the image. The aim of this study was to evaluate the quantitative accuracy of the CR scatter correction method. Secondary aims were to determine the influence of the CR scatter correction method on spatial resolution and image quality. Furthermore, the dependence of the scatter fraction on depth was determined.

Received Apr. 9, 1992; revision accepted Sept. 21, 1992
For correspondence and reprints contact: Mattheus G. Lötter, PhD, Biophysics Department, University of the Orange Free State, PO Box 339, Bloemfontein 9300, South Africa.

Theory

When mono-energetic gamma rays interact with a scintillation camera crystal the resultant energy spectrum exhibits a characteristic Gaussian shape which is determined by the intrinsic energy resolution of the detector assembly. When, in the absence of scattered photons, two narrow identical windows are placed adjacent to each other straddling the photopeak, the ratio (G) of the counts in the lower energy window (A) to that of the higher window (B) is close to one (Fig. 1A).

When the incident radiation also includes scattered photons the shape of the photopeak changes as a result of the reduced energy of these photons (Fig. 1B). The scatter components in the low and high energy windows are represented by C and D respectively. Although the ratio of the counts in the two windows for primary radiation ($G = A/B$) would still be the same, the ratio of total counts which includes both primary and scattered radiation in the windows $[(A + C)/(B + D)]$ will change (Fig. 1B). If these total counts in the low and high energy windows are represented by E and F respectively, the following equations result:

$$\text{Counts in lower window: } A + C = E \quad \text{Eq. 1}$$

$$\text{Counts in upper window: } B + D = F \quad \text{Eq. 2}$$

Constant ratio of counts in windows, excluding scatter:

$$A/B = G \quad \text{Eq. 3}$$

The problem is underdefined and an additional equation is needed to solve the set of variables.

Although the contribution of the scattered photons to the energy spectrum at different regions in an image is not constant, the assumption can be made that the intercept of the scattered radiation spectrum with the energy axis will be constant. This is due to the fact that scattering at small angles have little or no effect on the energy. The

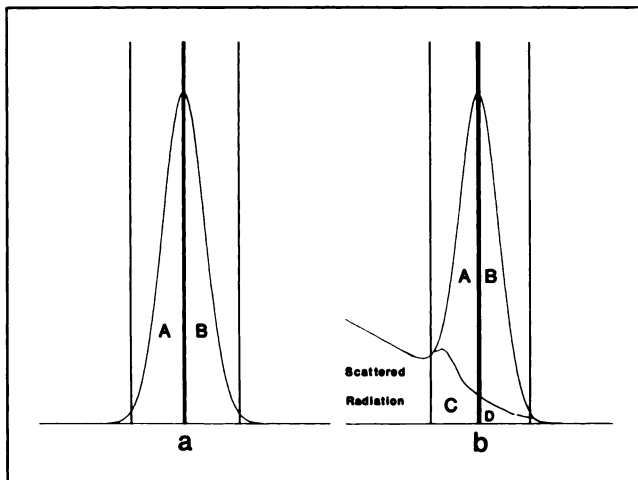


FIGURE 1. (A) Placement of windows on the photopeak when no scatter is present. (B) Approximation of the contribution made by scattered radiation to the two photopeak energy windows.

maximum detected energy of the scattered radiation and the photopeak is therefore the same (Fig. 1B). This assumption will only be valid if the full range of scattered photons is detected.

The fourth equation is based on the assumption that the relative shape of the energy spectrum of the scattered photons does not change significantly irrespective of the scatter contribution. This effect is evident when the shape of Monte Carlo simulations of the scatter component is studied (2). This is only true for mono-energetic radiation and for the narrow energy range of the photopeak. Scattered radiation originating from photon energies higher than the photon energy of interest would therefore be a complicating factor and can therefore not be corrected for by this method.

On the basis of the above assumption the fourth equation can be found, since the ratio of C/D would also be constant and independent of the relative size of the scatter contribution. Therefore:

$$\text{Constant ratio: } C/D = H. \quad \text{Eq. 4}$$

To find the value of $A + B$ expressed in the known quantities, Equations 1 to 4 are combined (Appendix A):

$$A + B = \frac{(G + 1)(HF - E)}{(H - G)}, \quad \text{Eq. 5}$$

with E and F the counts measured in the respective windows with scatter present, while the values of G and H have to be calibrated for the particular camera and photon energy.

To apply this formula to correct for the scatter contribution, it must be valid for each individual pixel of an image as well as for the counts generated in a region of interest (ROI). This is true since applying Equation 5 to a ROI gives:

$$\frac{(G + 1)(H\sum F_i - \sum E_i)}{(H - G)} = \sum_i \left[\frac{(G + 1)(HF_i - E_i)}{(H - G)} \right],$$

where E_i and F_i are the counts in the two windows for the i -th pixel and \sum_i is the summation over any number of pixels. The equation thus proves that it is equivalent to perform scatter correction first on a pixel-by-pixel basis and then sum over a region or to correct the sums of the ROI.

MATERIALS AND METHODS

The experiments were designed to determine the calibration values of G and H , evaluate the accuracy of quantitation when the CR scatter correction method is used and determine the effect of the correction method on image resolution.

Determination of G : The Nonscatter Photon Count Ratio

Although the value of G is theoretically equal to 1, in practice it may assume different values at various positions across the face of the camera. The G value was determined by placing a source containing 10 MBq [^{99m}Tc]pertechnetate in a 1-ml syringe at least

2 m in front of the open face of a General Electric 400 AT Starcam scintillation camera system. The syringe contained less than 0.1 ml of the radionuclide. Point source geometry could therefore be assumed. In order to minimize scatter it was ascertained that no object was within 0.5 m from either the source or the camera. Two images were acquired simultaneously using 10% energy windows with 5% offsets to both sides of the center of the photopeak. Imaging was terminated after a total of 5 million counts were collected. The low energy image was subsequently divided by the high energy image. The resultant image represented the individual pixel G values. The average and standard deviation of the G values were calculated. The variation in the average G value during the experimental period was also determined.

Determination of H: The Scatter Photon Count Ratio

The principle of the method to determine H is that if scatter is accurately eliminated, the counts obtained at different depths in an attenuating medium will undergo a single exponential decrease. When the logarithm of these counts is plotted against depth, the resulting straight line will have a slope equal to the attenuation coefficient for narrow beam geometry.

Data acquisition was performed using three 6-mm thick circular flat sources with diameters of 34, 85 and 169 mm respectively. Images were collected for 300 sec in 150 mm air and 10, 20, 30, 50, 100, 150 and 200 mm water using a water bath phantom fitted with an adjustable plexiglass rack. Counts from the two images of each source were determined by drawing a ROI to include all pixels within a 10% threshold value of the maximum count in each image. These counts were subsequently corrected for scatter using Equation 5. The G value calibrated before the measurement and an initial estimated H value of 3.0 was used. The subsequent scatter corrected counts were then fitted to a single exponential function and the corresponding attenuation coefficient obtained. Thereafter, the value of H was changed iteratively and the calculations repeated until the calculated attenuation coefficient corresponded to that for water and ^{99m}Tc photons, i.e., 0.01545 mm^{-1} (20). The measurements were repeated three times for each source. An average and standard deviation of H were subsequently calculated for all sources and measurements. This average value was used in all subsequent calculations as the calibrated H value.

Accuracy of Quantitation

To test the accuracy of quantitation, the correction for scatter was applied to the three circular flat sources imaged in water at the various depths mentioned previously. A ratio of the CR corrected counts (for each determination) to the corresponding counts obtained in 100 mm water was obtained for the three sets of data. To observe the improvement in quantitation with the CR scatter correction method, simple attenuation correction without scatter correction was also performed. The counts in the two 10% energy windows were summed and corrected for attenuation by using an effective attenuation coefficient of 0.012 mm^{-1} .

The Effect of the CR Scatter Correction Method on Resolution

The impact on image resolution with the CR scatter correction method was evaluated quantitatively using FWHM and FWTM values. Two capillary tubes were filled with ^{99m}Tc , placed 100 mm apart in a plane parallel to the collimator face and imaged

at 100 mm and 150 mm from the camera face in air as well as in water. A reference image was formed by summing the images from the two windows (resulting in a standard 20% window acquisition), while a CR scatter corrected image was also calculated using the calibrated G and H values. Count profiles were generated perpendicularly across the line sources at the same position for both images and FWHM and FWTM values calculated from the resultant curves.

Determination of a Scatter Fraction

From the formula for the CR scatter correction method, it follows that the fraction of photons scattered into the photopeak for a 20% energy window is given by (21-23):

$$\text{SF} = \frac{[(E + F) - (A + B)]}{A + B},$$

where SF is the scatter fraction. Scatter fraction was calculated for the three sets of data obtained from sources at different depths used in the evaluation of the accuracy of quantitation.

The Impact of Scatter Correction on Visual Image Quality

The effect of the CR scatter correction method on the quality of clinical images is demonstrated on bone and liver scans. The CR corrected images are compared to images obtained by adding the two 10% energy window images in each case which then correspond to an image from a 20% energy window. To minimize the effect of noise, an image corresponding to the scattered photons was calculated (14) and smoothed using a Hanning filter with a cut-off frequency of 0.8 cm^{-1} . The smoothed scatter image was then subtracted from the 20% energy window image to yield a primary photon image.

Statistical Analysis

The Student t-test was used to evaluate the influence of source size on the value of H ($p < 0.05$ was considered significant).

RESULTS

Nonscatter Photon Count Ratio G

The average G value was 0.94 for the useful field of view during the experimental period of 6 wk. The average G value varied by 3.0% during the experimental period while the average variation was 5.3% across the image.

Scattered Photon Count Ratio H

The average values for H obtained for the various source sizes were 2.38 ± 0.05 , 2.67 ± 0.17 and 2.87 ± 0.07 for the small, medium and large sources respectively. The H value of the small source differed significantly from those of the other two sources ($p < 0.05$). The average H value of all the sources was 2.64 ± 0.25 and was used in the calculations as the calibrated value.

Accuracy of Quantitation

The relative accuracy of quantitation when the CR scatter correction method was applied for the sources at different depths of water was compared to that when broad

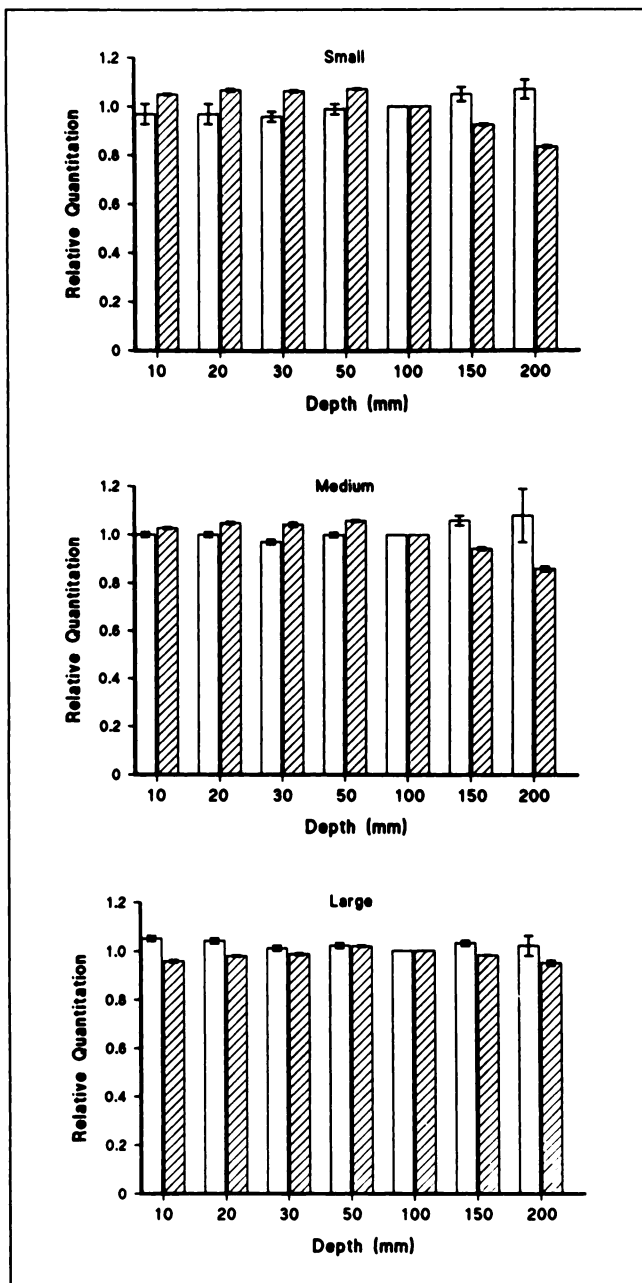


FIGURE 2. Accuracy of the CR scatter correction method compared to broad-beam attenuation correction for sources imaged at various depths in water. Values are normalized to those obtained in 100 mm water. Open bar = CR corrected count ratio and hatched bar = count ratio from broad-beam geometry.

beam attenuation correction without scatter compensation was used and is shown in Figure 2. A maximum difference of 8% (overestimation) with the CR method was obtained with the medium sized source at a depth of 200 mm (Fig. 2B) compared to the reference depth of 100 mm. The simple attenuation correction yielded a maximum difference of 17% (underestimation) with the small source at a depth of 200 mm (Fig. 2A). The superior accuracy of the CR scatter correction method is clearly demonstrated.

TABLE 1
Resolution Values for Line Sources Imaged in Air and in Water

	FWHM (mm)	FWTM (mm)
100 mm air	10.78 ± 0.20	18.39 ± 0.32
100 mm water	11.67 ± 0.02	22.53 ± 0.11
CR method	10.65 ± 0.05	18.01 ± 0.06
150 mm air	13.64 ± 0.01	23.55 ± 0.01
150 mm water	14.82 ± 0.05	32.73 ± 0.22
CR method	13.42 ± 0.08	22.78 ± 0.10

Effect on Resolution

The FWHM and FWTM resolution values for the line source profiles obtained in air and in water are given in Table 1. A 9.5% improvement in FWHM was obtained, while a maximum improvement of 30.4% in FWTM was achieved when the CR scatter correction method was applied to data measured at a depth of 150 mm water. The CR scatter correction method restored the resolution values obtained in water to those obtained in air.

Scatter Fraction

Results obtained when calculating the scatter fraction at different depths of water for the three sources are presented in Figure 3. The scatter fractions increased with depth and varied between 0.20 and 1.44.

Clinical Images

Examples of the influence of the CR scatter correction method on image quality are given in Figure 4. An improvement in contrast is clearly demonstrated on planar liver and bone images. However, noise was also increased as could be expected due to the subtraction of scattered counts. The reduction of noise as a result of smoothing the scattered photon image before subtraction is also demonstrated.

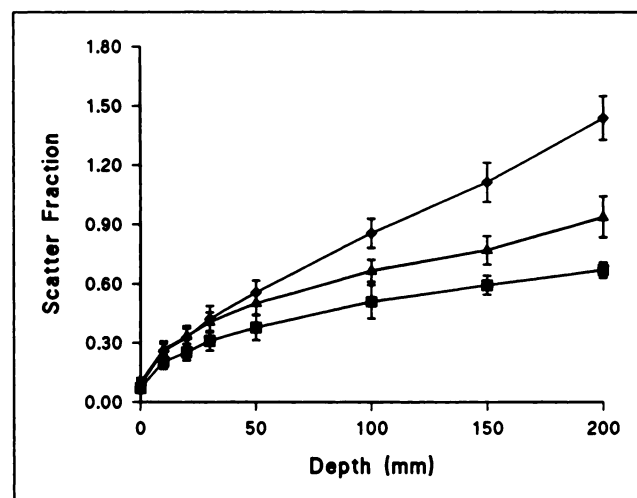


FIGURE 3. Variation of the scatter fraction with depth in a scattering medium for different source sizes. Square = small source, triangle = medium source and diamond = large source.

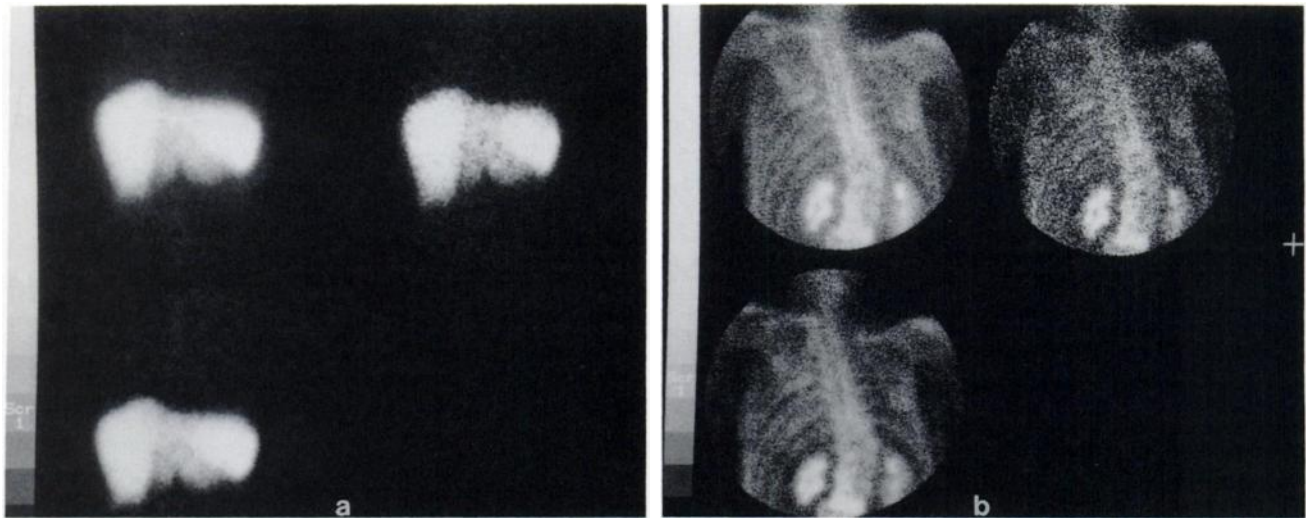


FIGURE 4. Examples of (A) liver and (B) bone images in patients. The top left images were acquired with normal 20% energy window, while CR scatter corrected images are shown on the

top right. The bottom left images were obtained after low-pass filtering of the scatter component.

DISCUSSION

In this study, it was shown that the CR scatter correction method can be successfully applied for the quantitation of activity in sources of different sizes and in different depths of water. Good agreement was obtained when the activity quantified with the CR scatter correction method at the different depths was compared to those obtained in 100 mm water. The maximum difference was 8%. When the simple exponential function with the broad beam attenuation coefficient was used, a maximum difference of 17% was obtained. This result confirmed that the CR scatter correction method yielded better quantitation than when broad beam attenuation correction was used.

The value of G will depend on the energy stability of the camera. Hademenos et al. (24) found that a drift of 0.5 keV could effect the G value by approximately 10% which corresponds to an error of roughly 10% in the final quantitation. They reported that the rotation of the camera through 360° caused a maximum drift in the value of G of 5%. Therefore it is important that the energy stability of a specific camera should be evaluated when the CR scatter correction method is used. We suggest that the G value should be determined immediately prior to the acquisition of the quantitation study.

The best way to investigate the effect of scatter on the value of H is to generate energy spectra using Monte Carlo techniques (2). These methods, however, are time-consuming and require special computing facilities. The size and the depth of the sources could influence the value of H and therefore the shape of the energy spectrum of the scattered photons. The H value measured for the small source was significantly lower than those of the other sources indicating that the accuracy of the method was to a limited degree dependent on source size. This is probably

due to the fact that the ROIs drawn for the larger sources will include photons scattered through all angles up to the angle corresponding to the energy of the lower level of the energy window. For smaller sources, the contribution of photons scattered through larger angles will be less. The corresponding energy spectrum of the smaller sources would contain fewer low energy photons. This would decrease the H value compared to that for larger sources. Although the dependence of the H value on source size contributed towards the inaccuracy in quantitation, this quantitation was acceptable.

Total breakdown of the CR scatter correction method could occur when only scattered photons and no primary photons are included in the ROI. In this situation, the smaller number of scattered photons in the upper energy window, F , relative to a larger number of photons in the lower window, E , will result in $HF < E$ (Equation 5), leading to negative pixel values in the image. This breakdown is of lesser importance since it would only apply to the region outside the edge of an organ and the influence of this breakdown can be excluded on a pixel-by-pixel basis by setting $A + B$ equal to zero whenever the ratio E/F exceeds the H value. However, the CR scatter correction method was primarily developed to be used for quantitation of radioactivity in an organ or ROI which contains primary as well as scattered photons.

The improvement in resolution, especially in the FWTM values of the line sources, has been clearly demonstrated. The restoration of the FWTM values at depths of 100 mm and 150 mm in water to the values that were obtained in air illustrated the efficiency of the method.

It was found that the application of the CR scatter correction method visually improved image contrast. Counting statistics did decrease as a result of the correction technique and resulted in a deterioration of image quality.

King et al. (14) recently introduced a dual-photopeak window method for scatter correction based on an identical data acquisition method but a different data processing algorithm. A scatter estimate image was obtained which, after low-pass filtering, was subtracted from the total image to yield an estimate of the primary photon image. We demonstrated that the quality of the CR corrected image could also be improved by performing similar low-pass filtering of the scatter image.

Monte Carlo simulations (21) and experimental measurements (22,23) showed that photons closer to the surface undergo less Compton scattering and yielded smaller scatter fractions. This variation in the scatter fraction could be demonstrated with the CR scatter correction method showing a clear dependence on depth and source size as indicated in Figure 3.

The CR method of scatter correction can be easily implemented and produces accurate results. It can be used in conjunction with the necessary attenuation correction to quantify radionuclide distributions in planar imaging. The CR scatter correction method can also be applied to SPECT, provided that the energy spectrum remains stable during rotation of the camera detector (25).

APPENDIX A

Method of Scatter Correction

The following four equations are used to derive a formula for $A + B$ in terms of the known values E through H :

$$A + C = E \quad \text{Eq. A1}$$

$$B + D = F \quad \text{Eq. A2}$$

$$A/B = G \quad \text{Eq. A3}$$

$$C/D = H. \quad \text{Eq. A4}$$

From Equation A3

$$A = BG \quad \text{Eq. A5}$$

therefore

$$A + B = B(G + 1). \quad \text{Eq. A6}$$

Also, from Equation A4

$$C = DH \quad \text{Eq. A7}$$

substituting Equations A5 and A7 in Equation A1 gives:

$$BG + DH = E. \quad \text{Eq. A8}$$

Eliminating D using Equations A2 and A8 gives:

$$BG - BH = E - HF,$$

therefore

$$B = \frac{(E - HF)}{(G - H)}.$$

Multiply by $(G + 1)$ on both sides:

$$B(G + 1) = \frac{(G + 1)(E - HF)}{(G - H)}$$

from Equation A6 therefore

$$A + B = \frac{(G + 1)(HF - E)}{(H - G)}.$$

REFERENCES

- Harris CC, Greer KL, Jaszczak RJ, Floyd CE Jr, Fearnow EC, Coleman RE. Technetium-99m attenuation coefficients in water-filled phantoms determined with gamma cameras. *Med Phys* 1984;11:681-685.
- Floyd CE, Jaszczak RJ, Harris CC, Coleman RE. Energy and spatial distribution of multiple order Compton scatter in SPECT: a Monte Carlo investigation. *Phys Med Biol* 1984;29:1217-1230.
- Lowry CA, Cooper MJ. The problem of Compton scattering in emission tomography: a measurement of its spatial distribution. *Phys Med Biol* 1987;32:1187-1191.
- Wu RK, Siegel JA. Absolute quantitation of radioactivity using the buildup factor. *Med Phys* 1984;11:189-192.
- Siegel JA, Wu RK, Maurer AH. The buildup factor: effect of scatter on absolute volume determination. *J Nucl Med* 1985;26:390-394.
- Siegel JA. The effect of source size on the buildup factor calculation of absolute volume. *J Nucl Med* 1985;26:1319-1322.
- Van Rensburg AJ, Lötter MG, Heyns A du P, Minnaar PC. An evaluation of four methods of ^{111}In planar image quantification. *Med Phys* 1988;15:853-861.
- Jaszczak RJ, Greer KL, Floyd CE, Jr., Harris CC, Coleman RE. Improved SPECT quantification using compensation for scattered photons. *J Nucl Med* 1984;25:893-900.
- Koral KF, Wang X, Rogers WL, Clinthorne NH. SPECT Compton-scattering correction by analysis of energy spectra. *J Nucl Med* 1988;29:195-202.
- Koral KF, Swailem FM, Buchbinder S, Clinthorne NH, Rogers WL, Tsui BMW. SPECT dual-energy-window Compton correction: scatter multiplier required for quantification. *J Nucl Med* 1990;31:90-98.
- Gilardi MC, Bettinardi V, Todd-Pokropek A, Milanese L, Fazio F. Assessment and comparison of three scatter correction techniques in single photon emission computer tomography. *J Nucl Med* 1988;29:1971-1979.
- Axelsson B, Msaki P, Israelsson A. Subtraction of Compton-scattered photons in single-photon emission computerized tomography. *J Nucl Med* 1984;25:490-494.
- Msaki P, Axelsson B, Dahl CM, Larsson SA. Generalized scatter correction method in SPECT using point scatter distribution functions. *J Nucl Med* 1987;28:1861-1869.
- King MA, Hademenos GJ, Glick SJ. A dual-photopeak window method for scatter correction. *J Nucl Med* 1992;33:605-612.
- Yanch JC, Flower MA, Webb S. A comparison of deconvolution and windowed subtraction techniques for scatter compensation in SPECT. *IEEE Trans Med Imag* 1988;7:13-20.
- DeVito RP, Hamill JJ, Treffert JD, Stoub EW. Energy-weighted acquisition of scintigraphic images using finite spatial filters. *J Nucl Med* 1989;30:2029-2035.
- Hamill JJ, DeVito RP. Scatter reduction with energy-weighted acquisition. *IEEE Trans Nucl Sci* 1989;36:1334-1339.
- Halama JR, Henkin RE, Friend LE. Gamma camera radionuclide images: improved contrast with energy-weighted acquisition. *Radiology* 1988;169:533-538.
- Maor D, Berlad G, Chrem Y, Soil A, Todd-Pokropek A. Klein-Nishina based energy factors for Compton free imaging (CFI) [Abstract]. *J Nucl Med* 1991;32:1000.
- Johns HE, Cunningham JR. *The physics of radiology*, 4th edition. Springfield, IL: Charles C. Thomas; 1983:723.
- Yanch JC, Flower MA, Webb S. Improved quantification of radionuclide uptake using deconvolution and windowed subtraction techniques for scatter compensation in single photon emission computed tomography. *Med Phys* 1990;17:1011-1022.
- Manglos SH, Floyd CE, Jaszczak RJ, Greer KL, Harris CC, Coleman RE. Experimentally measured scatter fractions and energy spectra as a test of Monte Carlo simulations. *Phys Med Biol* 1987;32:335-343.
- Knesaurek K. Two new experimental methods of calculating scatter fraction as a function of depth in scattering media: a comparison study. *Med Phys* 1992;19:591-598.
- Hademenos GJ, King MA, Ljungberg M, Morgan HT. The effects of uniformity on dual photopeak window scatter correction method. *J Nucl Med* 1992;33:962-963.
- Swailem FM, Koral KF, Rogers WL. Count-based monitoring of Anger-camera spectra—local energy shifts due to rotation. *Med Phys* 1991;18:565-567.